



**HAL**  
open science

## Hot and cool summers: Multiple equilibria of the continental water cycle

Fabio d'Andrea, Antonello Provenzale, Robert Vautard, Nathalie de Noblet-Decoudré

► **To cite this version:**

Fabio d'Andrea, Antonello Provenzale, Robert Vautard, Nathalie de Noblet-Decoudré. Hot and cool summers: Multiple equilibria of the continental water cycle. *Geophysical Research Letters*, 2006, 33 (24), 10.1029/2006GL027972 . hal-03134520

**HAL Id: hal-03134520**

**<https://hal.science/hal-03134520>**

Submitted on 8 Feb 2021

**HAL** is a multi-disciplinary open access archive for the deposit and dissemination of scientific research documents, whether they are published or not. The documents may come from teaching and research institutions in France or abroad, or from public or private research centers.

L'archive ouverte pluridisciplinaire **HAL**, est destinée au dépôt et à la diffusion de documents scientifiques de niveau recherche, publiés ou non, émanant des établissements d'enseignement et de recherche français ou étrangers, des laboratoires publics ou privés.



## Hot and cool summers: Multiple equilibria of the continental water cycle

Fabio D'Andrea,<sup>1</sup> Antonello Provenzale,<sup>2</sup> Robert Vautard,<sup>3</sup> and Nathalie De Noblet-Decoudré<sup>3</sup>

Received 8 September 2006; revised 20 October 2006; accepted 2 November 2006; published 20 December 2006.

[1] Large variations in soil water reserves and surface temperature over the continents are linked to a positive feedback between precipitation and soil moisture. This mechanism can generate bimodal distributions of soil moisture. Here, we show that bimodality results from the existence of multiple equilibria in the continental water balance, considering the coupled system including the upper soil layer and the atmospheric planetary boundary layer. This mechanism is described with an idealized box model, that includes convergence and divergence of moisture fluxes, convection, precipitation and evapotranspiration. The existence of two equilibria is associated with the variation of precipitation efficiency, which depends on convection intensity. The two regimes correspond to realistic values of climatic variables associated with mean wet or dry summers, and can persist for the whole summer season when forced by a stochastic moisture convergence flux. This suggests that a key role for midlatitude continental summer climate is played by the continental soil water content. **Citation:** D'Andrea, F., A. Provenzale, R. Vautard, and N. De Noblet-Decoudré (2006), Hot and cool summers: Multiple equilibria of the continental water cycle, *Geophys. Res. Lett.*, 33, L24807, doi:10.1029/2006GL027972.

### 1. Introduction

[2] During the unprecedented August 2003 heatwave in Europe, temperature exceeded its usual value by 5 standard deviations [Schär *et al.*, 2004]. This event had dramatic effects on vegetation productivity [Ciais *et al.*, 2005], air quality [Vautard *et al.*, 2005] and health [World Health Organization, 2003], as well as on the socio-economic activities, ranging from agriculture to energy consumption [Fink *et al.*, 2004]. As a consequence, the interest in the problems of climate extrema in midlatitudes has increased in the last few years. Of particular importance is the possibility of an increase of their frequency because of global climate change.

[3] Observational studies [Chang and Wallace, 1987] and General Circulation Model (GCM) studies [Oglesby and Erickson, 1989; Ferranti and Viterbo, 2006; Huang *et al.*,

1996] have shown the importance of the continental water budget for summer temperature and precipitation. Due to a positive feedback between soil moisture and precipitation/cloud cover, the continental climate undergoes persistent dry or wet spells. A dry soil favours sensible heat flux relative to latent heat flux in the surface energy budget. The heat excess and soil water deficit results in fewer clouds, less rain and greater demand for evapotranspiration which further depletes the soil water reservoir. A dry soil also inhibits the triggering of convective precipitation [Schär *et al.*, 1999], leading to more anticyclonic weather.

[4] Using station data from the midwest of the United States, D'Odorico and Porporato [2004] (hereinafter referred to as DP) showed that the probability distribution of summer moisture in the upper 50 cm soil layer has a bimodal shape. Summers have high likelihood to be either in a wet or a dry state. They also found a correlation between soil moisture and rainfall, which they interpreted as sign of a positive feedback mechanism. They proposed a statistical model for this feedback, similar to those of Rodriguez-Iturbe *et al.* [1991] or Entekhabi *et al.* [1992], where the frequency of rainfall depends on soil moisture through a regression calculated from the observations. Based on this regression, rainfall is stochastically forced in their water cycle model, leading to a bimodal distribution of soil water content. A bimodal distribution in this model naturally originates from the state-dependent stochastic dynamics, also known as "multiplicative noise" [see, e.g., Porporato and D'Odorico, 2004, and references therein].

[5] In this paper, we propose a physical mechanism for the existence of a bimodal probability distribution of soil moisture. Our approach is based on complementing a soil model similar to that used by DP with a simple representation of the moist thermodynamics of the atmospheric planetary boundary layer (PBL), which includes a simple parametrization of moist convection. This coupled soil-atmosphere model predicts the existence of multiple equilibria in the water balance of the atmospheric PBL and the upper soil layer.

[6] In the next section the model is briefly described, for technical details the reader is referred to the auxiliary material.<sup>1</sup> Section 3 describes the results obtained, and discussion and conclusions are given in section 4.

## 2. Model Description

### 2.1. Thermodynamic Equations

[7] The interaction between the atmospheric PBL and the surface hydrology is provided by an idealized box model of

<sup>1</sup>Laboratoire de Météorologie Dynamique, Institut Pierre-Simon Laplace, Ecole Normale Supérieure, Paris, France.

<sup>2</sup>Institute of Atmospheric Sciences and Climate, Consiglio Nazionale delle Ricerche, Torino, Italy.

<sup>3</sup>Laboratoire des Sciences du Climat et de l'Environnement, Institut Pierre-Simon Laplace, Commissariat à l'Energie Atomique, Centre National de la Recherche Scientifique, Université de Versailles Saint-Quentin-en-Yvelines, Gif sur Yvette, France.

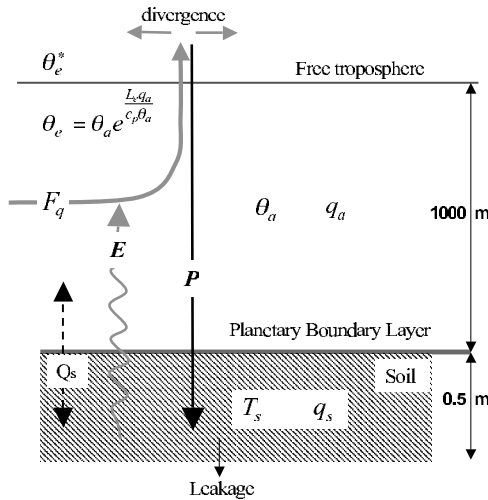


**Figure 1.** Schematics of the box-model, the formula to compute the equivalent potential temperature of the PBL  $\theta_e$  is repeated in the upper left corner. Thick arrows show input and output water fluxes. Gray represents air humidity, black represents liquid water.

the continental water cycle. The geometry of the model is schematized in Figure 1. It includes a 1000 m high atmospheric layer, and a 0.5 m deep soil layer, as in DP. In both media, temperature and humidity are prognostic variables, interacting by exchanges of heat, and exchanges of water by precipitation and evapotranspiration. This gives four prognostic variables; the four evolution equations are the following:

$$\rho c_p h_a \frac{\partial \theta_a}{\partial t} = Q_s + \epsilon_a \epsilon_s \sigma T_s^4 - \rho c_p h_a \frac{\partial \Delta \tilde{\theta}_a}{\partial t} + \frac{1}{\tau_a} (\theta_a^* - \theta_a) \quad (1)$$

$$\rho h_a \frac{\partial q_a}{\partial t} = E - \rho h_a \frac{\partial \Delta \tilde{q}_a}{\partial t} + F_q \quad (2)$$

$$\rho_s c_{ps} h_s \frac{\partial T_s}{\partial t} = F_{rad} - Q_s - \epsilon_s \sigma T_s^4 - L_e E \quad (3)$$

$$w_0 h_s \frac{\partial q_s}{\partial t} = P - E - L(q_s) \quad (4)$$

[8] In (2), the potential temperature of the atmospheric PBL  $\theta_a$  is forced by (left to right on the r.h.s.) the surface sensible heat flux  $Q_s$ , the infrared radiation from the ground, and the cooling rate due to convection. In the cooling term,  $\Delta \tilde{\theta}_a$  is different from zero only when convection occurs. Convection is assumed to take place whenever the PBL becomes statically unstable with respect to the free troposphere (see section 2.2 below). When convection occurs, the PBL and the free troposphere are assumed to mix and the variables  $\theta_a$  and  $q_a$  are correspondingly modified. The PBL temperature is also relaxed to a fixed external temperature  $\theta_a^* = 22^\circ\text{C}$  (last term on the r.h.s. of (2), corresponding to heat exchange due to transport and mixing). The relaxation has a timescale of  $\tau_a = 3$  days; our results are not very sensitive to this relaxation term. Table 1 provides a description of the main symbols, while the detailed calculation of the fluxes, evapotranspiration and precipitation is given in the auxiliary material. The values of the parameters are generally taken from work by *Laio et al.* [2001] or *Rodriguez-Iturbe and Porporato* [2004] for continental midlatitudes.

[9] The evolution of air humidity  $q_a$  (equation (3)) is driven by three terms. The second term on the r.h.s. represents the drying due to convection that mixes the moister air of the PBL with the drier air of the free troposphere. Part of this water is delivered to the soil as precipitation (see next two sections). We consider two source terms, evapotranspiration  $E$ , and a lateral moisture input term  $F_q$ , which is due to the large-scale mass field convergence. Atmospheric water (see the arrows in Figure 1), comes into the box model through this term, is lifted into the free troposphere by convection, and then is either precipitated or evacuated by flow divergence. If the model is thought to represent a general location in central Europe or inland USA,  $F_q$  represents an influx of maritime air from the west (Pacific or Atlantic oceans) or from the south (Gulf of Mexico or Mediterranean). The value of  $F_q$  is fixed so as to close the water budget. We use a mean value of  $10^{-8} \text{ s}^{-1}$  (approximately equivalent to 0.8 mm of water per day), but the behavior of the system has been tested for values ranging from a divergence of 1 mm of water per day to a convergence of 3 mm per day. The dependence of the model behavior on the value of  $F_q$  is discussed at length below.

[10] Soil temperature  $T_s$  is forced by the energy balance between incoming net radiation,  $F_{rad}$  in equation (3), outgoing infrared radiation, latent heat uptake by evapotranspiration and sensible heat flux  $Q_s$  as in (2).  $F_{rad}$

**Table 1.** Key Model Parameters and Their Values

Symbol	Meaning	Value	Units
$F_{rad}$	Net radiation at surface	450	$\text{W m}^{-2}$
$L_e$	Specific latent heat of Evaporation	$2.501 \cdot 10^6$	$\text{J Kg}^{-1}$
$R$	Ideal gas constant	287	$\text{J kgK}^{-1}$
$c_{pa}$	Air specific heat	1000	$\text{J kg}^{-1} \text{K}^{-1}$
$c_{ps}$	Soil specific heat	1000	$\text{J kg}^{-1} \text{K}^{-1}$
$h_a$	Thickness of the atmospheric boundary layer	1000	m
$h_s$	Depth of the soil active layer	0.5	m
$w_0$	Soil water holding capacity	1500	$\text{kg m}^{-3}$
$\epsilon_a$	Blackbody absorptivity of the PBL	0.3	
$\epsilon_s$	Blackbody emissivity of the Earth	0.8	
$\rho$	Air density	1	$\text{kg m}^{-3}$
$\rho_s$	Soil density	1800	$\text{kg m}^{-3}$

is assumed constant; its dependence on a representation of could cover has been tested and does not change substantially the results below.

[11] Equation (4) is the same as in DP. The quantity  $q_s$  represents the relative soil moisture with respect to saturation. Actual soil moisture is obtained by multiplying  $q_s$  by the soil water holding capacity  $w_0$ , and the depth of the active soil layer  $h_s$ . The results described below depend very weakly on the choice of  $w_0$  and  $h_s$ . The variation in  $q_s$  (equation (4)) is the result of the balance between precipitation P, evapotranspiration E and leakage L at the bottom of the active layer. The term P represents precipitation minus runoff. The exact formulation of all these terms is described in the auxiliary material.

## 2.2. Convection Parameterization

[12] The model includes a very simple parameterization of convection. The stability of the air column is assumed to depend only on the difference between the moist enthalpy of the PBL and that of the free troposphere above (see Figure 1). We assume that the equivalent potential temperature of the free troposphere has a fixed value  $\theta_e^*$ . At all timesteps we compute the equivalent potential temperature of the PBL,

$$\theta_e = \theta_a e^{\frac{Lc_p q_a}{\theta_a}}. \quad (5)$$

If  $\theta_e$  is less than  $\theta_e^*$ , the column is stable and no convection occurs. Conversely, if  $\theta_e > \theta_e^*$ , we assume that the column is convectively unstable.

[13] When convection occurs, the updraft cools and dries the PBL, until its equivalent potential temperature reaches  $\theta_e^*$  and convective equilibrium is restored. This procedure is similar to the convective adjustment scheme once used in general circulation models [Glickman, 2000]. The PBL height being fixed, there is no representation of entrainment. Both drying and cooling reduce equivalent potential temperature, according to its definition (5). In this simplified parameterization, the drying and cooling terms in equations (2) and (3) are obtained by assuming that before and after convection the PBL relative humidity stays the same. This allows us to express the two terms separately as a function of moist enthalpy  $c_p (\theta_e - \theta_e^*)$  (K. Emanuel, personal communication, 2006). The assumption of conservation of relative humidity is a crucial physical hypothesis for the results described below. Although after a single storm relative humidity can be locally increased by the convective downdraft associated to evaporating rain, it quickly relaxes towards its reference value, that is set by large-scale radiation and evapotranspiration balance. Our parameterization of convection is a representation of the bulk effect of a convectively active period in a large area, rather than that of an individual storm.

[14] The assumptions described above lead to the following formulae (see the system of equations (A-1)–(A-2) in the auxiliary material):

$$\Delta \tilde{\theta}_a = \frac{\theta_e - \theta_e^*}{1 + \frac{Lc_p}{\theta_a} q_{rel} \delta q_{sat}}, \quad (6)$$

$$\Delta \tilde{q}_a = q_{rel} \delta q_{sat} \Delta \tilde{\theta}_a, \quad (7)$$

where the term  $\delta q_{sat}$  in (7) is the Clausius-Clapeyron law linearized with respect to temperature, and  $q_{rel}$  is the relative humidity.

[15] Convective cooling and drying are assumed to take place immediately, time derivatives in the r.h.s. of (2) and (3) are substituted by the terms  $\frac{\Delta \tilde{\theta}_a}{\delta t}$  and  $\frac{\Delta \tilde{q}_a}{\delta t}$  and the parameter  $\delta t$  is set equal to the timestep of the model (1 hour).

[16] The parameter  $\theta_e^*$  is taken equal to 300°K. The results reported below do not change significantly for a reasonable range of  $\theta_e^*$ .

## 2.3. Precipitation

[17] The water subtracted from the PBL by the convective updraft is lifted into the free troposphere above. We assume that a fraction of this water precipitates locally, and the rest is lost by moisture flux divergence in the upper troposphere. The definition of this fraction — the precipitation efficiency — is one of the crucial physical hypotheses of this work; we assume that it is a function of the intensity of convection.

[18] If convection is weak, and thus the water updraft is weak, e.g. below 1 mm/day, we assume that a cloud is formed that is then transported out of the domain with little rain. Conversely, if the convection is very intense, a greater fraction of water is precipitated. This physical mechanism is in agreement with the observation of Schär *et al.* [1999], who showed by a regional modelling study of European summer that the precipitation efficiency is correlated with soil moisture. In their case, the precipitation efficiency was expressed in terms of rate of recycling of water, i.e. the ratio between precipitation and all the water entering a domain, including large scale convergence and local convection. Depending on the regional location and dry/wet periods this varied between 0 and 0.8.

[19] In our parameterization, at any time the precipitation rate is given by  $f \rho h_a \frac{\Delta \tilde{q}_a}{\delta t}$ , where  $f$  expresses the precipitation efficiency of the convection and  $\rho h_a \frac{\Delta \tilde{q}_a}{\delta t}$  is the convective updraft. If  $\rho h_a \frac{\Delta \tilde{q}_a}{\delta t}$  is less than 1 mm/day, precipitation efficiency is low,  $f = 0.2$ . If  $\rho h_a \frac{\Delta \tilde{q}_a}{\delta t}$  is larger, i.e. more than 3 mm/day, almost all water precipitates,  $f = 0.9$ . Between the two,  $f$  is joined smoothly, see Figure 2. The thresholds and values chosen for  $f$  are inspired by Schär *et al.* [1999], however different choices do not qualitatively change the results obtained. We will return to the importance of this mechanism in the discussion below.

## 3. Multiple Water Balance Equilibria

[20] For realistic values of the parameters, the simplified model has two stable equilibria; this is illustrated in Figure 3. Figure 3 is obtained by integrating the model starting from various initial soil moisture conditions (from 0 to 1) and stopping the integration when equilibrium is attained. In Figures 3a–3d, the x-axis reports the initial condition on  $q_s$ , and the y-axis shows the final – equilibrium – value of the model variables. The initial values of the three other prognostic variables are kept the same.



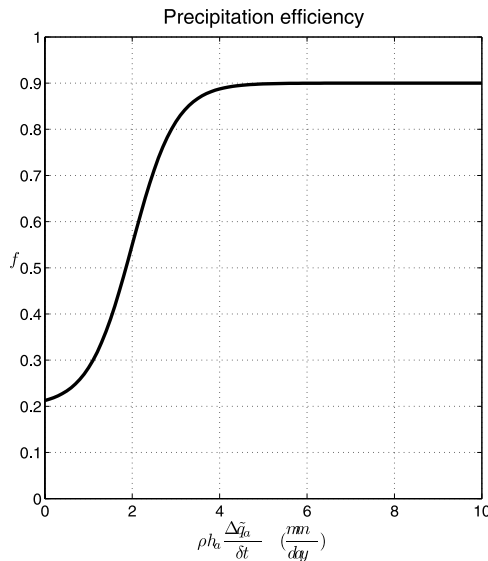


**Figure 2.** Precipitation efficiency as a function of the moisture updraft expressed in mm/day.

[21] The *dry* steady state is reached for initial conditions of soil humidity less than 0.32. Associated with this equilibrium, elevated soil temperature (26°C) and air temperature (24.5°C) are registered (Figure 3a). Both air specific humidity and soil moisture have low values, soil moisture lying just above the wilting point (Figure 3b). High sensible heat flux from the ground heats up the PBL (Figure 3c) and precipitation and evaporation are very low, below 1 mm/day (Figure 3d).

[22] The other state, the *wet* state, has much cooler conditions for a continental summer. The mean air temperature is much lower (about 16°C), and precipitation is high with almost 4 mm/day average, which is comparable to the observed mean values, see e.g. Figure B11 of the ERA-40 atlas [Källberg *et al.*, 2005]. Sensible heat flux is much smaller. High precipitation stabilizes soil moisture slightly above field capacity (0.58), and the excess water is eliminated by bottom leakage, hence the difference between evaporation and precipitation (Figure 3d).

[23] We have not detected any periodic or chaotic behavior of the model solutions. A detailed exploration of the model configuration and of the initial conditions indicates that the system is very sensitive to variations in the initial value of soil moisture, while it is relatively less sensitive to initial perturbations in the other dynamical variables.

[24] In the equilibrium integrations above, the value of  $F_q$  is fixed at 0.8 mm/day.  $F_q$  is a critical parameter in our model and we can extend the analysis by computing the equilibria for different values of it. When varying  $F_q$  over a wider range of values the system undergoes a hysteresis, as shown in Figure 4a. In this plot, only air temperature and soil moisture are shown but the other two prognostic variables, and also heat fluxes, precipitation and evapotranspiration display the same behavior. It can be seen that the region in which the two stable equilibria exist at the same time is about 0.7 mm/day wide and includes the mean value chosen in the equilibrium integrations above. The values of mean temperature and soil moisture in the two equilibrium branches do not vary much with  $F_q$ ; for

example temperature in the dry state can vary by 4°C, while the difference between the two equilibria is about 10°C.

[25] In order to estimate realistic values for the mean and variability of  $F_q$ , we computed the value of moisture flux convergence from ECMWF reanalysis data (not shown). The data were vertically integrated between 1000 and 850 hPa, and averaged over a region including most of continental France and Germany (0–10°E and 45–50°N lat/lon intervals). The mean value is around zero, with large spatial variations. The standard deviation is around 3 mm/day. These values correspond to upper limits for  $F_q$  in our model, since this parameter represents only part of the total vertically integrated moisture convergence (the other part is the divergence in the free troposphere).

[26] In order to simulate the impact of synoptic flow variability on the variability of the moisture flux convergence that actually drives our model, stochastic runs were performed using random values for the parameter  $F_q$ . The integration is very long (210<sup>5</sup> days). Every 10 days a new value of  $F_q$  is drawn from a flat distribution whose limits are the same as in Figure 4a: from –0.8 to 2.6 mm/day. Reasonable changes of the distribution amplitude and of the persistence time of  $F_q$  do not change the results.

[27] With this forcing, the model produces a bimodal distribution of soil moisture as in DP. In Figure 4b, a 15000-day-long portion of the evolution of  $q_s$  is shown. The soil moisture oscillates around the dry or the wet states and sometimes undergoes sudden transitions between the two. This is confirmed in the histogram in Figure 4c, which is in qualitative agreement with the bimodal distribution that DP

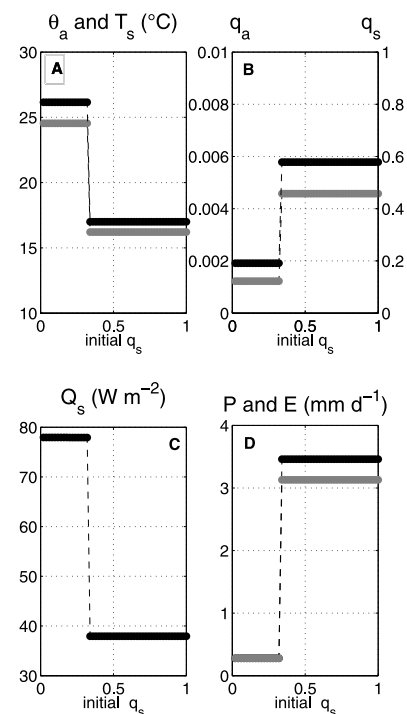


**Figure 3.** Equilibrium states as a function of the initial condition on soil moisture. (a) Air temperature (gray) and soil temperature (black). (b) air humidity in kg of water per kg of air (gray) and soil moisture expressed in fraction with respect to soil saturation (black). (c) Sensible heat flux. (d) Precipitation (black) and evapotranspiration (gray).

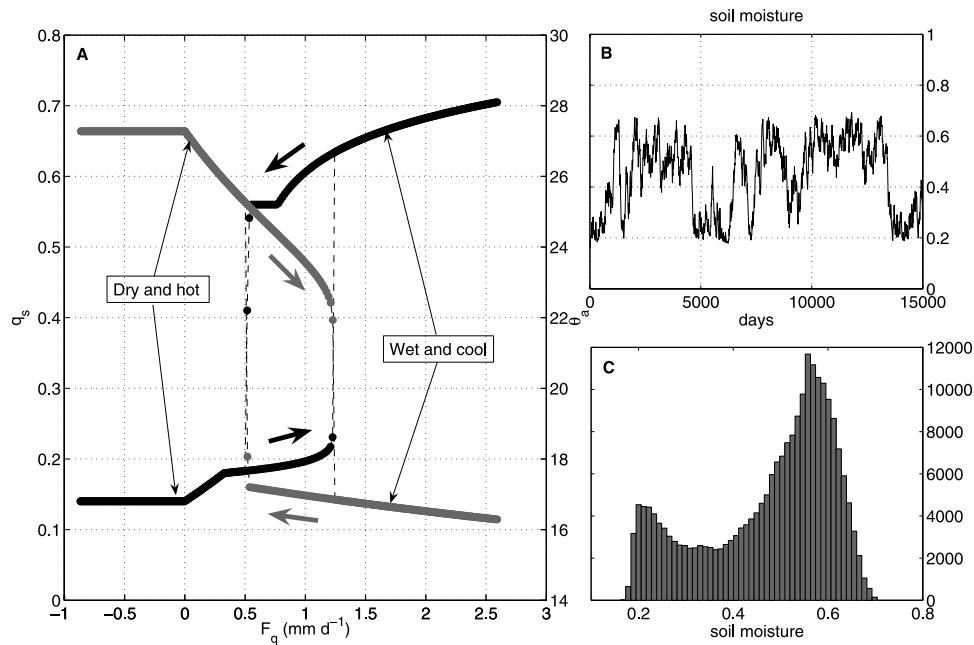


**Figure 4.** Sensitivity to the flux convergence  $F_q$ . (a) Values of PBL temperature (gray) and soil moisture (black) as a function of the  $F_q$ , expressed in  $\text{mmd}^{-1}$ . The branches corresponding to the dry state are attained by increasing values of  $F_q$  and the wet branches for decreasing values. Arrows mark the sense of the hysteresis cycle. (b) Time evolution of soil moisture in a 15000-day-long section of the stochastic run of the model. (c) Histogram of the values of  $q_s$  of the whole integration.

(see their Figure 3) computed from observed data. The other variables of the model also display bimodal or skewed probability density distributions (not shown).

[28] The long integration above does not obviously represent a realistic time evolution. It is produced by a very long integration of the model, while in reality we should consider many repetitions of a summer-long (around 150 days) time series. The model behavior suggests that it is more likely that one summer will be in one of the two states and remain there, than that a transition would happen during the season. This can be seen from Figure 4b, where the typical residence times in one regime is well above 150 days. Of course the simplicity of the model does not allow to overstate this result. Indeed there have been examples of “transitions” in the observed summer climate, a notable one being summer 2006 in Europe. Still, the initial condition on soil moisture at the beginning of the season is a key factor in determining which state, dry or wet, the summer will be likely to be in. This is in agreement with initialization studies such as those of *Ferranti and Viterbo* [2006] and *R. Vautard et al.* (Summertime European heat and drought waves follow wintertime Mediterranean rainfall deficit, submitted to *Geophysical Research Letters*, 2006).

#### 4. Discussion and Conclusions

[29] In this paper we advance a physical explanation for the observed bimodal distribution of soil moisture in mid-latitude summer. We formulate a 0-dimensional continental water balance model that includes the main energetic processes at the surface and in the planetary boundary layer (PBL), and a simplified representation of convection. This

model displays two stable equilibria. Depending on the soil water content at the beginning of the season, summers can be in one of the two states, with a low probability of transition to the other state during the season.

[30] Despite the simplicity of the model, the two stationary states bear realistic values of air temperature, humidity and precipitation, which can be associated to respectively cool/rainy or hot/dry summers. Dry summers are hot owing to the fact that reduced evapotranspiration leads to reduced cooling by latent heat flux. High soil temperatures are reached and the soil heats the atmospheric PBL by sensible heat flux. Differences in heat flux of  $50 \text{ Wm}^{-2}$  between hot and cool summers have been observed in Europe [*Zaitchik et al.*, 2006], similarly to our Figure 3c.

[31] The equilibria are maintained by a positive feedback between soil moisture and precipitation. Summer rains occur through the accumulation of moisture by large-scale convergence and by local recycling by convection. In the dry case, moisture convergence does not compensate for the drought created by the evapotranspiration leading to higher temperature, less convection and therefore less precipitation efficiency.

[32] In the model, water enters through convergence of lateral moisture fluxes in the PBL and is evacuated into the free troposphere. It is recycled by evapotranspiration and rain. We use a relation between the rate of recycling of water and the soil moisture inspired by that of *Schär et al.* [1999], but precipitation efficiency is assumed to depend on the intensity of convection only. The physical validity of this assumption is a crucial point of our work that needs further investigation. The nature of precipitation efficiency and its dependence on the physics of convection systems

and on the microphysics of clouds has indeed been topic of scientific enquiry since the 50's. Recent work shows its dependence on the relative humidity of the atmospheric PBL, that is in total agreement with our assumption [Market *et al.*, 2003, and references therein]. It must also be stressed that the results presented here are robust to changes in the functional form of the precipitation efficiency shown in Figure 2. Different choices of its upper and lower limit values and of the threshold lead to moderate changes in the values and the stability properties of the two stationary states, and in the soil moisture value of the saddle point between the two. As long as the efficiency increases with the intensity of convection, two stationary states are found.

[33] The main control parameter of our system is the external moisture flux,  $F_q$ . When this parameter is slowly varied and its values encompass the range of system bistability, the model undergoes a hysteresis cycle between the two stable states. When  $F_q$  is varied stochastically, the system jumps from one stable equilibrium to the other producing the bimodal probability density as was found by DP in observed data. Bimodality in continental soil moisture can thus be obtained by a coupling between convection and soil processes. It takes place because of additive noise forcing a system that has multiple equilibria. This physically-based mechanism extends the “multiplicative noise” approach of DP or Entekhabi *et al.* [1992] among others, where multimodality arises from the prescribed dependence of the noise on the state.

[34] Clearly, many physical processes that are also likely to affect the soil-PBL dynamics and equilibria are not present in our simplified model. These include the dependence of soil surface albedo on moisture, the effect of clouds in shading solar radiation, the dependence of the greenhouse effect on air humidity, and the dynamical response of vegetation, and thus of evapotranspiration, to soil humidity. Future work will address some of these issues. Another direction of development is the spatial extension of the model, which allows us to include the spatial dependence of the different parameters, as well as mixing and transport in the PBL.

[35] Large variations in summer temperature and soil moisture, such as the heat wave and drought of August 2003 in Europe, is generated by the nonlinear dynamics of the coupled soil-PBL system, which includes highly nonlinear processes such as moist convection and evapotranspiration. The understanding of these processes is fundamental for the prediction of the occurrence of extreme events, and their impacts under climate change conditions.

[36] **Acknowledgments.** The authors wish to thank the following colleagues for advice and interesting discussion: Sandrine Bony, Rodrigo Caballero, Francesco d'Ovidio, Jean-Philippe Duvel, Kerry Emanuel, Nick

Hall, Masa Kageyama, Francesco Laio, Amilcare Porporato, Joe Tribbia, Nicolas Viovy, Pascal Yiou, Jeffrey Weiss.

## References

- Chang, F. C., and J. M. Wallace (1987), Meteorological conditions during heat waves and droughts in the United States Great Plains, *Mon. Weather Rev.*, *115*, 1253–1269.
- Ciais, P., *et al.* (2005), Europe-wide reduction in the primary productivity caused by the heat and drought in 2003, *Nature*, *437*, 529–533.
- D'Odorico, P., and A. Porporato (2004), Preferential states in soil moisture and climate dynamics, *Proc. Natl. Sci. Acad. U.S.A.*, *101*, 8848–8851.
- Entekhabi, D., I. Rodriguez-Iturbe, and R. L. Bras (1992), Variability in large-scale water balance with land surface-atmosphere interaction, *J. Clim.*, *5*, 798–813.
- Ferranti, L., and P. Viterbo (2006), The European summer of 2003: Sensitivity to soil water initial conditions, *J. Clim.*, *19*, 3659–3680.
- Fink, A. H., T. Bruecher, G. C. Leckebusch, A. Krueger, J. G. Pinto, and U. Ulbrich (2004), The 2003 European summer heatwaves and drought—Synoptic diagnosis and impacts, *Weather*, *59*(8), 209–216.
- Glickman, T., *et al.* (Ed.) (2000), *Glossary of Meteorology*, 2nd ed., 850 pp., Am. Meteorol. Soc., Boston, Mass.
- Huang, J., H. M. Van den Dool, and K. P. Georgarakos (1996), Analysis of model calculated soil moisture over the United States (1931–1993) and applications to long-range temperature forecasts, *J. Clim.*, *9*, 1350–1362.
- Källberg, P., P. Berrisford, B. Hoskins, A. Simmons, S. Uppala, S. Lamy-Thrépaut, and R. Hine (2005), ERA-40 atlas, *ERA-40 Proj. Rep. Ser. 19*, Eur. Cent. for Medium-Range Weather Forecasts, Reading, U. K.
- Laio, F., A. Porporato, L. Ridolfi, and I. Rodriguez-Iturbe (2001), Plants in water controlled ecosystem: Active role in hydrologic processes and response to water stress II. Probabilistic soil moisture dynamic, *Adv. Water Resour.*, *24*, 707–723.
- Market, P., S. Allen, R. Scofield, R. Kuligowski, and A. Gruber (2003), Precipitation efficiency of warm season midwestern mesoscale convective systems, *Weather Forecasting*, *18*, 1273–1285.
- Oglesby, R. J., and D. J. Erikson (1989), Soil moisture and the persistence of North American drought, *J. Clim.*, *2*, 124–129.
- Porporato, A., and P. D'Odorico (2004), Phase transition driven by state dependent poisson noise, *Phys. Rev. Lett.*, *92*, 110601.
- Rodriguez-Iturbe, I., and A. Porporato (2004), *Echohydrology of Water Controlled Ecosystems*, Cambridge Univ. Press, New York.
- Rodriguez-Iturbe, I., D. Entekhabi, and R. L. Bras (1991), Nonlinear soil moisture dynamics at climate scales: 1. Stochastic analysis, *Water Resour. Res.*, *27*, 1899–1906.
- Schär, C., D. Luthi, and U. Beyerle (1999), The soil-precipitation feedback: A process study with a regional climate model, *J. Clim.*, *12*, 722–741.
- Schär, C., P. L. Vidale, D. Luthi, C. Frei, C. Haberli, M. A. Liniger, and C. Appenzeller (2004), The role of increasing temperature variability in European summer heatwaves, *Nature*, *427*, 332–336.
- Vautard, R., C. Honoré, M. Beekmann, and L. Rouil (2005), Simulation of ozone during the August 2003 heat wave and emission control scenarios, *Atmos. Environ.*, *39*, 2957–2967.
- World Health Organization (2003), The health impacts of 2003 summer heat-waves, briefing notes for the delegations of the fifty-third session of the WHO (World Health Organization) regional committee for Europe, 12 pp., Geneva, Switzerland.
- Zaitchik, B. F., A. K. Malcalady, L. R. Bonneau, and R. B. Smith (2006), Europe's 2003 heat wave: A satellite view of impacts and land-atmosphere feedbacks, *Int. J. Climatol.*, *26*, 743–770.
- F. D'Andrea, Laboratoire de Météorologie Dynamique, IPSL, Ecole Normale Supérieure, Paris, France. (dandrea@lmd.ens.fr)
- N. De Noblet-Decoudré and R. Vautard, Laboratoire des Sciences du Climat et de l'Environnement IPSL, CEA/CNRS/UVSQ, F-91191 Gif sur Yvette, France.
- A. Provenzale, Institute of Atmospheric Sciences and Climate, CNR, I-101133 Torino, Italy.

## Auxiliary material: Details of model equations

### a. Sensible heat flux

Sensible heat flux is given by the aerodynamic bulk formula

$$Q_s = \rho c_p C_D |\bar{u}_s| C_D (T_s - \theta_a),$$

where the mean wind  $\bar{u}_s$  is taken equal to  $6 \text{ m s}^{-1}$ . The flux is by convention positive when heating the atmosphere and cooling the soil.

### b. Evapotranspiration

The formula for evapotranspiration is taken from Laio et al (2001), however we modulate the maximum evaporation efficiency by a term taking into account the saturation deficit of the atmosphere. In detail,

$$E = E' \frac{q_{Sat} - q_a}{q_{Sat}},$$

where  $q_{Sat}$  is the saturation humidity at a given air temperature, and:

$$E' = \begin{cases} 0 & \text{for } q_s \leq q_h \\ \frac{q_s - q_h}{q_w - q_h} E_w & \text{for } q_h \leq q_s \leq q_w \\ E_w + \frac{q_s - q_w}{q^* - q_w} (E_{Max} - E_w) & \text{for } q_w \leq q_s \leq q^* \\ E_{Max} & \text{for } q_s \geq q^* \end{cases}$$

Where  $q^*$ ,  $q_w$ , and  $q_h$  are the soil humidity of maximum plant efficiency, the wilting point and the hygroscopic point respectively.  $E_{Max}$  and  $E_w$  are the values of unconstrained evapotranspiration at full plant efficiency, and the value of evaporation at wilting point, i.e. the evaporation from the soil. Refer to Tab.1 in the article text for the values.

### c. Leakage

The leakage formula is taken from Laio et al (2001) and it represents the rapid loss of water from the surface layer by gravity-induced water motions towards the deeper soil layers, that takes place when the soil moisture is larger than the field capacity  $q_{fc}$ :

$$L(q_s) = K_s \frac{e^{\beta(q_s - q_{fc})} - 1}{e^{\beta(1 - q_{fc})} - 1}.$$

Here,  $K_s$  is the saturated hydraulic conductivity of the ground,  $\beta$  is a fitting parameter and  $q_{fc}$  is the field capacity of the soil. See Tab.1.

### d. Precipitation rate and runoff

The precipitation rate  $P'$  is a fraction of the total moisture updraft  $\Delta\tilde{q}$  (see text). The precipitated water  $P$  that actually penetrate the soil layer is equal to  $P'$  minus the runoff: if the amount of precipitation in a given time exceeds the saturation of the soil layer, the leftover water is lost from the PBL-soil system.



$$P = \begin{cases} P' & \text{for } P' \leq \frac{1 - q_s}{\delta t} \\ \frac{1 - q_s}{\delta t} & \text{for } P' \geq \frac{1 - q_s}{\delta t} \end{cases}$$

*e. Convection*

To obtain formulae (6) and (7) in the article text we consider the variation of air moist enthalpy needed to restore convective equilibrium:

$$\theta_e - \theta_e^* = \Delta\tilde{\theta}_a + \frac{L_e}{c_p} \Delta\tilde{q}_s, \quad (\text{A-1})$$

and we impose the conservation of relative humidity  $q_{rel}$  at the first order:

$$q_{rel} \delta q_{sat} \Delta\tilde{\theta}_a = \Delta\tilde{q}_a, \quad (\text{A-2})$$

where the term  $\delta q_{sat}$  in (A-2) represents the derivative of the Clausius-Clapeyron law with respect to temperature. Solving the system of equations (A-1, A-2) gives (6) and (7).

Symbol	Meaning	Value
$C_D$	Bulk aerodynamic drag coefficient	0.008
$E_{Max}$	Maximum Potential Evapotranspiration	$6 \cdot 10^{-5} \text{ Kg m}^{-2} \text{ s}^{-1}$
$E_w$	Evapotranspiration at wilting point	$5 \cdot 10^{-6} \text{ Kg m}^{-2} \text{ s}^{-1}$
$q_w$	Wilting point	0.18
$q_h$	Hygroscopic point	0.14
$q^*$	Maximum plant efficiency point	0.46
$q_{fc}$	Field capacity	0.56
$K_s$	Saturated hydraulic conductivity	0.03 $\text{m d}^{-1}$
$\beta$	parameter of water retention	14.

Table 1: Other model parameters and their values.